Bubble-Turbulence Interaction in Binary Fluids

2011 J. Phys.: Conf. Ser. 318 092011

(http://iopscience.iop.org/1742-6596/318/9/092011)

Bubble-Turbulence Interaction in Binary Fluids

Battista F., Froio M., Picano F., Gualtieri P., Casciola C.M.

Dipartimento di Ingegneria Meccanica e Aerospaziale, Sapienza University of Rome, via Eudossiana 16, 00184, Italy

E-mail: francesco.battista@uniroma1.it

Abstract. Multiphase flows represent a central issue in many natural, biological and industrial fields. For instance, liquid jets vaporization, petroleum refining and boiling, emulsions in pharmaceutical applications, are all characterized by a disperse phase, such as solid particles or liquid bubbles, which evolve in a Newtonian carrier fluid. Features such as the global evaporation rates of liquid fuels in air or the homogeneity of the emulsions are controlled by the finest interaction details occurring between the two phases. In this paper we study the rising motion of a bubble induced by buoyancy in a viscous fluid. Usually this issue is tackled by tracking the bubble interface by means of sharp interface methods. However this approach requires "ad hoc" techniques to describe changes in the topological features of the deforming interface and to enforce the mass preservation. Here the problem is addressed by using a different philosophy based on a diffuse interface method, that allows a straightforward analysis of complex phenomena such as bubbles coalescence and break up without any numerical expedient. The model we adopt, funded on a solid thermodynamical and physical base, relies on the Cahn-Hilliard equation for the disperse phase, see Cahn & Hilliard (1958) and Elliott & Songmu (1986).

1. Introduction

Multiphase flows are common in many natural, biological and industrial systems. Typical examples are liquid fuel jets in different kind of engines, petroleum refining and boiling, emulsions in pharmaceutical applications, chemical reactors. In all these cases a Newtonian fluid carries a disperse phase, such as solid particles or liquid droplets, which gives rise to a complex and intriguing dynamics. Among the different aspects of the general problem concerning turbulence in multiphase flows, the present paper focuses on the issue of the rising (falling) of the bubbles (droplets), their deformation and break-up and the turbulent fluctuations thereby generated. The overall importance of the topic is proved by the great number of dedicated numerical and experimental studies. In Grace *et al.* (1976) and Bhaga & Weber (1981) Reynolds (Re), Eötvös (Eo) and Morton (Mo) numbers are identified as the proper dimensionless parameters which control the dynamics and determine shape and terminal velocity of a rising (falling) bubbles (droplets). Further experiments have shown, see e.g Tomiyama *et al.* (2002), the crucial role of the initial bubble shape on the successive rising dynamics in pure or contaminated water when surface tension is determinant and the bubble Reynolds number is small.

Concerning numerical approaches, most studies were based on potential flow theory, see e.g. Oguz & Prosperetti (1993), which provides a reasonable description of the physics when slip occurs at the bubble surface. The improvements of numerical techniques and the increased computational capabilities of super-computers recently allowed for finely resolved simulations of rising bubbles (or falling droplets) aimed at understanding and revealing more detail on flow structures and dynamical mechanism. In Ryskin & Leal (1984) the authors perform one of the first numerical simulations of rising

bubbles addressing the bubble dynamics in the steady state regime while in Unverdi & Tryggvason (1992) a three-dimensional simulation extends the analysis to the transient phase. The results show very good agreement with the experimental data in regimes characterized by small shape deformations and rising velocities. However the numerics, based on front tracking algorithms, become computationally heavy when the interface get substantially entangled. Actually tracking and capturing the interface involves several numerical and algorithmic issues especially when a topology change occurs (e.g. the bubble break-up). In addition these procedures employ mathematical expedients related to the interpolation of the thin interface which may have non trivial consequences on the accuracy of the method. In this context, level set and volume-of-fluid method or their combination are worth mentioning as further numerical improvements for the treatment of the thin gas/liquid interface (Ohta *et al.*, 2005).

In this paper we investigate essentially the same kind of dynamics by using the Navier-Stokes equations coupled with the Cahn-Hilliard equation (Cahn & Hilliard (1958)). The latter allows to mimic a binary system of two immiscible liquids by introducing a phase variable φ which discriminates between the two pure fluids, $\varphi = \pm 1$, while ranging from -1 to $+1$ across the thin interface.

The relevant system of equation is summarized in the next section. In § 3 we describe the numerical algorithm and the simulation parameters. A comparison of our results with the data obtained by Bhaga & Weber (1981) and our main contributions are presented in § 4, while § 5 provides a final discussion on numerical method and physical results.

2. Mathematical model

In diffuse interface methods the dynamics of two immiscible fluids is reproduced by somewhat artificially thickening the interface. The consistency of the model relies upon a suitable thermodynamical description where an additional contribution to the free energy density of the two pure fluids accounts for the interface surface energy. According to Cahn & Hilliard (1958) a phase field variable $\varphi \in [-1, 1]$ is employed to describe the two phases. The free energy density is given by

$$f(\varphi, \nabla\varphi) = \frac{1}{2}\lambda \left|\nabla\varphi\right|^2 + f_0(\varphi) \tag{1}$$

where the contribution proportional to the square of the phase variable gradient through the phenomenological coefficient λ accounts for non local effects due to the interatomic interactions between the two phases. The double-well potential $f_0 = \lambda/(2\varepsilon^2)(\varphi^2 - 1)^2$ takes care of the existence of two stable states corresponding to the pure fluids. The phenomenological coefficient, $\lambda/(2\varepsilon^2)$, is expressed in terms of the interfacial energy coefficient λ and the additional parameter ε which is a measure of the interface thickness. Relaxation of the free energy

$$F = \int_\Omega f(\varphi, \nabla\varphi) d^3\mathbf{x} \tag{2}$$

towards its minimum is described by the Cahn-Hilliard equation

$$\frac{\partial\varphi}{\partial t} + \mathbf{u}\cdot\nabla\varphi = \frac{S^2}{Cn\,Ca}\nabla^2\mathcal{G} = \frac{S^2}{Cn\,Ca}\nabla^2\left(\varphi^3 - \varphi - Cn^2\nabla^2\varphi\right) \tag{3}$$

where $\mathcal{G}$ is the chemical potential, $Cn = \varepsilon/\ell$ is the Cahn number, ratio of the interface thickness ε and a typical macroscopic scale ℓ, $Ca = \mu U_c/\sigma$ is the Capillary number which estimates the ratio of viscous to capillary forces, with μ the dynamic viscosity of the carrier fluid ("background phase"), U_c the macroscopic velocity and σ the surface tension. Finally the dimensionless number $S = \sqrt{M\mu}/\ell$ accounts for the Onsanger mobility coefficient M, here taken constant. For the Cahn-Hillard equation, taken saparately from the momentum balance of the fluid (modified Navier-Stokes equation), S controls the characteristic time scale. As well known, the two contributions to the free energy density have

opposite effects: the first one $(\varphi^3 - \varphi)$ promotes the formation of uniform patches of pure fluid, thereby leading to the formation of interfaces. The second one $(Cn^2\nabla^2\varphi)$ penalizes the interface itself, where the phase variable gradient is significant, thus contributing to reduce the extension of the interface. In physical terms, the interface is extremely thin in standard conditions (order of few nanometers) hence the Cahn number it is expected to be very small. Simple dimesional consideration reported below show that S is also extremely small Yue *et al.* (2010).

The flow is assumed isothermal, both fluid are incompressible and the only density variations occur across the interface since the density depends φ. Under these hypothesis the Cahn-Hillard equation (3) is coupled to the incompressible Navier Stokes equations,

$$\begin{aligned} \nabla \cdot \mathbf{u} &= 0 \\ \frac{\partial \mathbf{u}}{\partial t} + \mathbf{u} \cdot \nabla \mathbf{u} &= -\nabla p + \frac{1}{Re}\nabla^2 \mathbf{u} + \frac{1}{Re\, Ca\, Cn}\mathcal{G}\nabla\varphi + \frac{1}{Fr^2}\left(1 - \frac{\rho(\varphi)}{\rho_0}\right)\hat{\mathbf{g}}\,. \end{aligned} \tag{4}$$

In the momentum balance equation $Re = U_c \ell \rho_0/\mu$ is the Reynolds number and $Fr = U_c/\sqrt{g\ell}$ is the Froude number with $\mathbf{g} = g\hat{\mathbf{g}}$ the gravitational acceleration. As anticipated, the density depends on the field variable and the ratio between local, $\rho(\varphi)$, and carrier phase density, ρ_0, generates the buoyancy term. A linear dependence captures the essential physics, se e.g. Celani *et al.* (2009),

$$\rho(\varphi) = \frac{1-\varphi}{2}\rho_0 + \frac{1+\varphi}{2}\left(\rho_0 - \Delta\rho\right)$$

and assuming $\rho_0 - \Delta\rho \ll \rho_0$ the buoyancy term reads

$$\frac{1}{Fr^2}\frac{1+\varphi}{2}\hat{\mathbf{g}}\,.$$

Surface tension is described by the distributed force proportional to chemical potential times the phase gradient, $\mathcal{G}\nabla\varphi$, which accounts for the momentum exchange between the two phases. The complete model can be shown to be thermodynamically consistent for a system of two immiscible fluids.

3. Methodology

The equations presented in the section § 2 are integrated in a triply periodic box with dimension $[L_x \times L_y \times L_z] = [2\pi \times 2\pi \times 4\pi]$ by means of a semi-implicit Fourier pseudo-spectral algorithm which allows to easily integrate the high order spatial derivative terms in implicit form, with no time step restriction for stability. A classical approach, see also Gualtieri *et al.* (2002), is used for the momentum balance equation, with the non linear convective term written in the Lagrange form and explicitly treated during the time integration while keeping the dissipative term implicit. Solenoidality of velocity is achieved by projection on the divergence free subspace. Since all scalars whose gradient enters the momentum coupling between the phases,

$$\left(\varphi^3 - \varphi - Cn^2\nabla^2\varphi\right)\nabla\varphi = \nabla\left(\frac{\varphi^4}{4} - \frac{\varphi^2}{2}\right) - Cn^2\nabla^2\varphi\nabla\varphi\,, \tag{5}$$

can be gathered in a modified pressure $\tilde{p} = p + \varphi^4/4 - \varphi^2/2$ which is taken care by projection, surface tension reduces to the last term in (5).

Concerning the Chan-Hillard equation (3), after a careful analysis of its particular form, the same basic semi-implicit approach is used. Specifically, the convective term and the Laplacian term on the right hand side, $\nabla^2(\varphi^3 - \varphi)$, are explicit while the forth order term, $\nabla^4\varphi$, is implicit, to avoid unaffordable stability time step limitations. Note that both the non linear, $\nabla^2\varphi^3$, and the linear term, $\nabla^2\varphi$, are taken

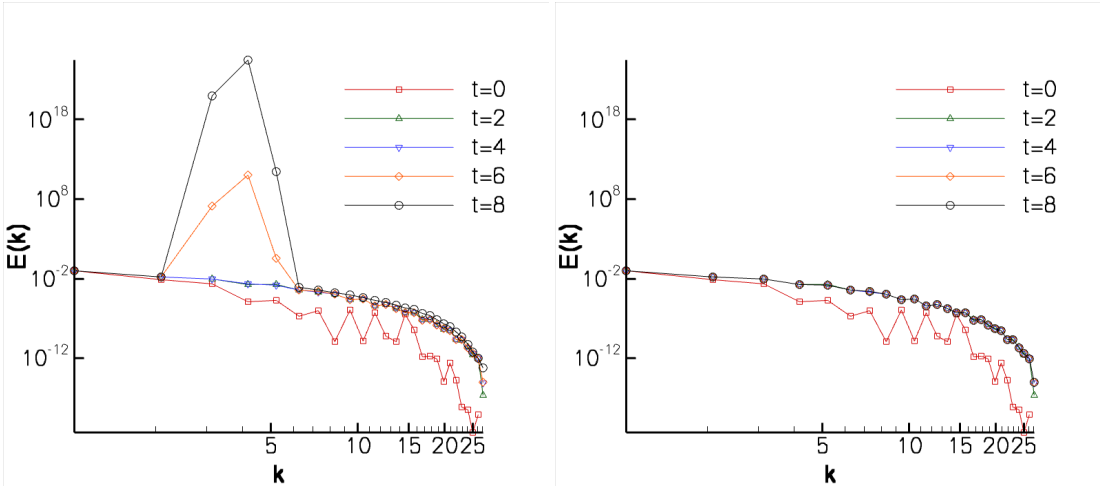

Figure 1. Phase field spectra for the isolated Cahn-Hillard equation. Left panel: partially implicit treatment of the Laplacian term; right panel: explicit treatment of the Laplacian term.

together in explicit form, even though the latter could have been easily incorporated in the implicit part of the algorithm. Figure 1 show that separating the two contribution is indeed detrimental for stability. The figure shows the phase field spectra at different time steps taken from two numerical solutions of the Cahn-Hilliard equation with no coupling to the momentum equation. The left panel refers to the case where the two terms are split between implicit and explicit part of the algorithm, the right panel to the case where both are explicit. The equation is solved in a $[L_x \times L_y \times L_z] = [2\pi \times 2\pi \times 2\pi]$ triply-periodic domain on a $[N_x \times N_y \times N_z] = [48 \times 48 \times 48]$ grid. Starting from the same initial condition, the interface between the two phases evolves towards a spherical shape, consistently with the minimum energy principle. The low-wavenumber numerical instability of the first approach, left panel, is apparent with an unphysical growth of the modes in a band around $k = 4$. The simultaneous explicit treatment keeps stable for the entire evolution reaching the expected steady state solution.

In the one-dimensional case and only for specific boundary conditions the Cahn Hilliard equation is known to conserve the global volume fraction, see Furihata (2001) and Liu *et al.* (2005). In the fully three dimensional case addressed here, we explicitly checked the total mass conservation by tracking its evolution in time of all the simulations presented. It is also important to keep in mind that the maximum principle does not hold implying that the phase field φ is not strictly constrained to the range $-1 < \varphi < +1$, see Liu *et al.* (2005).

Before discussing our results, a few more considerations on the values of the dimensionless are in order. Capillary and Cahn numbers can be easily estimated by direct experiments measuring surface tension and interface thickness. Concerning $S = \sqrt{M\mu}/\ell$ the situation is less clear due to the presence of the Onsanger mobility coefficient M. For interfaces between two fluid phases the mobility is extremely difficult to address directly by experiments and is more the result of an effective modeling of the interface dynamics. Its suggested values are extremely small, Yue *et al.* (2010), as could be concluded by the following dimensional reasoning. The quantity ρM can be considered the characteristic time-scale associated with the interface dynamics. Let us introduce the diffusive fluid time scale associated to the interface thickness ε, $\rho\varepsilon^2/\mu$. The interesting dynamics occurs when coupling exists between the two, $\rho M \simeq \rho\varepsilon^2/\mu$. This leads to the estimate of the Onsanger Mobility number as

$$M \sim \frac{\varepsilon^2}{\rho\nu} \sim 1 \times 10^{-15} \frac{\mathrm{m^3 s}}{\mathrm{kg}},$$

where a water/air interface ws considered.

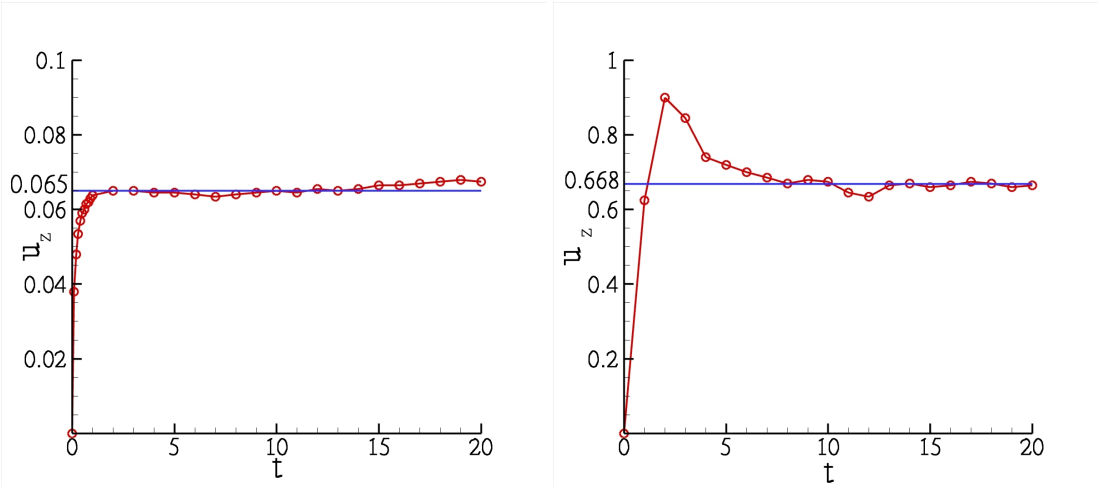

Figure 2. Bubble rising velocity variation depending on non dimensional time. Left panel: first simulation S1, right panel: second simulation S2. Parameters in table 2

Concerning the Cahn number, since the interface thickness is on the nanometer scale, for a bubble with diameter $D = 10^{-3}m$ it follows $Cn = \varepsilon/\ell \sim 10^{-6}$. It is clear that the interface is too thin to be tackled by numerical simulations, given the enormously large number of collocations point that would be necessary necessary for its resolution. Nonetheless the Cahn-Hiliard model could still be though off as a viable way to mimic the thin interface using an artificial numerical thickening. This amounts to consider Cn as large as possible before unphysical effects emerge in the solution. Going the other way around, one should progressively decrease Cn until the solution become independent of the specific value of the Cahn number, thus identifying the so-called so called *sharp interface limit*.

4. Results & perspectives

The results of our diffuse-interface direct numerical simulation of a rising bubble are here compared against experimental data by Bhaga & Weber (1981) and numerical data obtained with the sharp interface tracking method discussed in Hua & Lou (2007). These authors use the Morton $Mo = g\mu_2^4/(\rho_2\sigma^3)$ and the Eötvös $Eo = g\ell^2\rho_2/\sigma$ numbers (definitions recalled in the introduction) as control parameters, see table 1. To match our parameters we assume $Fr = 1$ and find Reynolds and Capillary number by the relations $Re = \sqrt[4]{Eo^3/Mo}$, $Ca = \sqrt[4]{MoEo}$, table 2. In addition we set $S = 10^{-4}$ and $Cn = 10^{-2}$.

The two simulations are performed in a $[L_x \times L_y \times L_z] = [2\pi \times 2\pi \times 4\pi]$ domain with $[N_x \times N_y \times N_z] = [384 \times 384 \times 768]$ collocation points. The characteristic dimension of the cell grid is $\Delta x = 1.6 \times 10^{-2}$, corresponding to three collocation points within the interface. Figure 3 shows an instantaneous

test	Eo	Mo	Re	v_{lim}
S1	8.67	711	0.078	0.069
S2	32.2	0.00082	55.3	0.663

Table 1. Parameters of the two cases discussed in Bhaga & Weber (1981) and Hua & Lou (2007). The last column gives the terminal rising velocity of the bubble, Hua & Lou (2007)

.

configuration of the rising bubbles (right column) in comparison with the experimental data of Bhaga & Weber (1981) (left column) and numerical results provided by Hua & Lou (2007) (middle column).

test	Re	Ca	Fr	v_{lim}
S1	0.078	8.86	1.	0.065
S2	55.3	0.4	1.	0.668

Table 2. Set of parameters used in the two simulations described in the text. v_{lim} in the last column is the terminal rising velocity, see table 1 for comparison.

The agreement with both reference cases is quite reasonable and the terminal rising velocity v_{lim}, last column of tables 1 and 2, shows that the correspondence is quite acceptable also in quantitative terms.

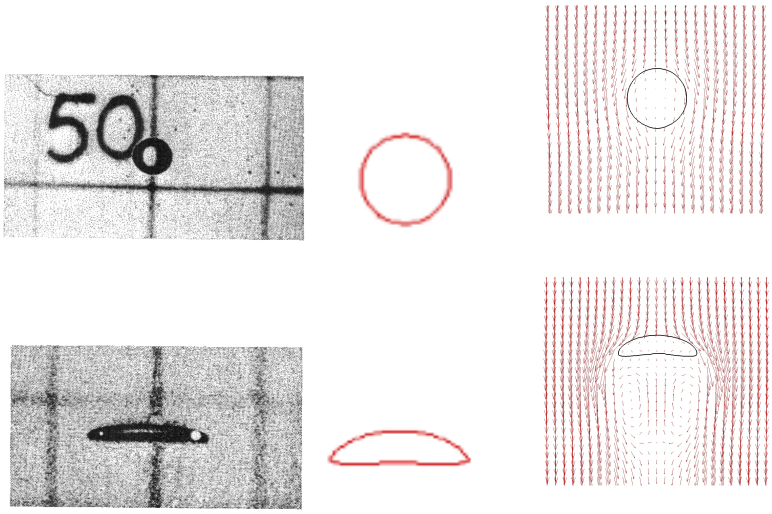

Figure 3. Comparison between the experiment of Bhaga & Weber (1981) (left panels), the numerical results of Hua & Lou (2007) (middle panels) and the present simulations (right panels). The black solid line in the right panels marks the iso-level $\varphi = 0$. Vectors (red in electronic version) provide the local fluid velocity. The parameters are summarized in the table 1 with same top to bottom arrangment.

The bubble of simulation S1 raises at a very small terminal velocity with an almost constant shape. This is a low Reynolds number case: the impinging flow is too weak to overcome suface tension and the bubble shape is unaffected. The velocity vectors (top left panel of figure 3) show that the flow is quite similar to a Stokes flow with only a very small wake behind the bubble. The bubble velocity evolution is presented in figure 2 where the velocity increases progressively until reaching the pateau corresponding to the terminal velocity. In the last phases a slow but evident increase of the rising velocity is observed. This is an artificial effect of the periodic boundary conditions, when the bubble starts interacting with the wake produced by its own forward image.

With the parameters of the second simulation, S2, the bubble dynamics is entirely different also as concerning the bubble shape, figure 3. Since the Reynolds number is larger and the capillary number is almost the same of simulation S1 the flow velocity is significantly increased and the bubble deformed from its initial shape. Figure 4 (left panel) presents the time evolution of the bubble shape. In this case the flow around the bubble is substantially different from the Stokes flow observed in case S1. Indeed, behind the initial spherical bubble the two recirculating regions induce a positive velocity insisting on the stagnation point behind the bubble and brake the forwards-aft symmetry of the previous case.

In the first stages when the bubble is accelerated from rest the velocity in the recirculation regions is larger than the rising velocity. The bubble is then forced to assume the characteristic ”cup” shape

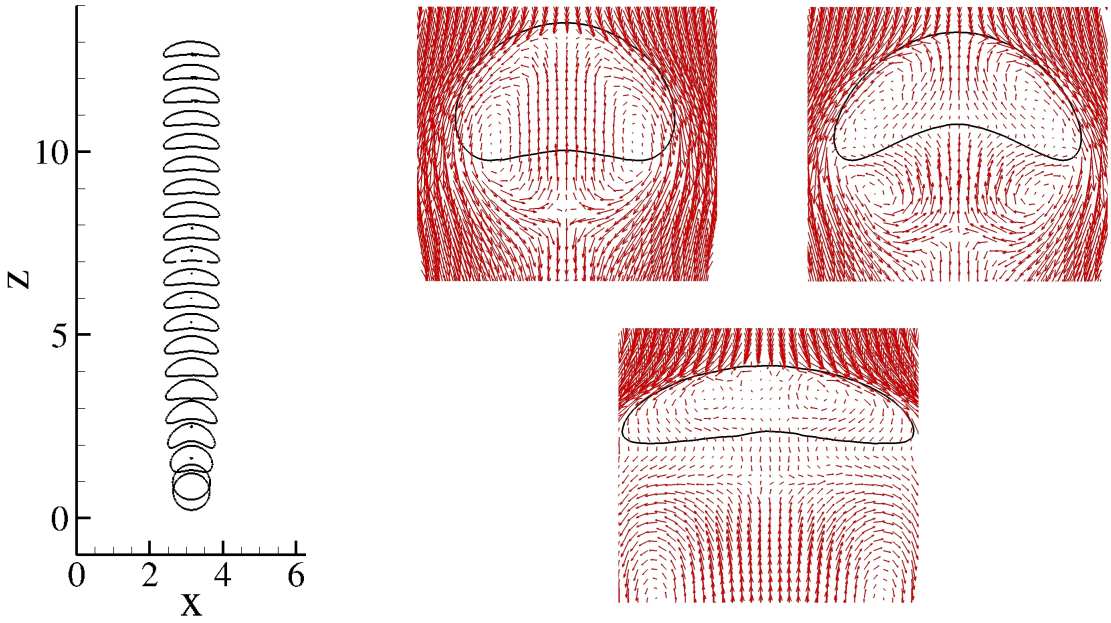

Figure 4. Left panel: bubble shapes along the time evolution under the effects of the buoyancy and the drag force for case S2, see table 2. Right panel: Instantaneous bubble shape (solid line) and fluid velocity field (red arrows) at three different time istants: $t = 2$ (top-left panel), $t = 3$ (top-right panel), $t = 15$ (bottom panel).

apparent in the right panel of figure 4. As the rising velocity increases, it overcomes for a while the terminal raising velocity achieved at later times, right panel of figure 2. During this phase the fluid velocity difference between front and aft of the bubble and the strain associated with the recirculating regions induce a further deformation of the bubble which assumes a disk-like shape. In these conditions the drag exerted on the bubble increases and the bubble eventually slows down to its terminal velocity, see figure 2 (right panel).

As preliminary simulations show, a further increase of the Reynolds number and a decrease of the Capillary number lead to larger deformations of the air-water interface which easily evolves towards more complex structures with significant topological changes. In such conditions the Cahn-Hilliard equations are in principle still able to describe the dynamics. However, to avoid numerical artifacts, it is necessary to increase substantially the number of collocation points, to correctly capture the small-scale interface corrugation and the bubble break-up in the correct *sharp interface limit*.

5. Final remarks and discussion

Numerical simulations of a buoyancy-dominated raising bubble has been performed based on the Cahn-Hillard model for binary flows. This diffuse interface approach adopts a phase variable φ that ranges from $\varphi = +1$ to $\varphi = -1$ in the thin interface between the two phases. The method is excellent for the simulation of binary flows in presence of strong interface deformation and works also in case of topological changes associated to bubble break-up. As a drawback, the need to reach the *sharp interface limit* to capture the correct dynamics of actual fluid-fluid interfaces compels to adopt very thin interfaces (small Cahn number). This requirement results in strong limitations especially in three-dimensional simulations when the interface topology becomes extremely complex and, simultaneously, the bubble dimensions are small compared with the integral scale of the system. So-far this limited the adoption of the Cahn-Hillard model coupled with the Navier-Stokes equation system to two-dimensional cases.

Here we have attempted a three-dimensional simulation for the simple case of a single rising bubble in otherwise still fluid. The dynamics of rising bubbles is a well known problem widely discussed in the literature and is an interesting test case to evaluate potentiality and drawbacks of the diffuse interface method. The coupled Navier-Stokes/Cahn-Hilliard system has exploited its potential in the data we have discussed showing good qualitative and quantitative agreement with previous results available in the literature, Bhaga & Weber (1981) and Hua & Lou (2007). Indeed, we were able to explain the interaction of fluid structures and interface through the distributed surface tension that provides the momentum source of the Navier-Stokes equations.

Although only a small range of Capillary and Reynolds numbers were investigated, the overall impression is that the approach could be pushed to study turbulence induced bubble/droplet break-up in a turbulent flow. Often, however, the situation is in principle easier to handle that in the extreme case of bubble break up. In equilibrium, bubble/droplet dimensions, turbulence intensity and interface parameters are expected to result in characteristic values of the bubble/droplet Reynolds and Capillary numbers far away from the critical values corresponding to large shape deformations and break-up, conditions in principle much easier to handle from the numerical point of view. Concerning future perspectives of this preliminary attempt, on one side we intend to address the turbulence intensity required to achieve bubble break-up and coalescence as a function of surface tension and bubble size. On the other side, we are interested in analyzing the local turbulence modification induced by bubble deformations in the context of two-way coupling modeling of multiphase flows. Both aspects are crucial in different areas of applications of multiphase flows, e.g. understanding droplet formation/coalescence in turbulent systems of different nature and liquid jet break-up modeling of use in a number of technological applications.

Acknowledgments

The work was supported by the Standard HPC-2011 Grant (N. std11-455) providing CPU time and storage at CASPUR High Performance Computing Center.

References

BHAGA, D. & WEBER, ME 1981 Bubbles in viscous liquids: shapes, wakes and velocities. *Journal of Fluid Mechanics* **105** (-1), 61–85.

CAHN, J.W. & HILLIARD, J.E. 1958 Free energy of a nonuniform system. i. interfacial free energy. *The Journal of Chemical Physics* **28**, 258.

CELANI, A., MAZZINO, A., MURATORE-GINANNESCHI, P. & VOZELLA, L. 2009 Phase-field model for the rayleigh–taylor instability of immiscible fluids. *Journal of Fluid Mechanics* **622** (-1), 115–134.

ELLIOTT, C.M. & SONGMU, Z. 1986 On the cahn-hilliard equation. *Archive for Rational Mechanics and Analysis* **96** (4), 339–357.

FURIHATA, D. 2001 A stable and conservative finite difference scheme for the cahn-hilliard equation. *Numerische Mathematik* **87** (4), 675–699.

GRACE, JR, WAIREGI, T. & NGUYEN, TH 1976 Shapes and velocities of single drops and bubbles moving freely through immiscible liquids. *Chemical Engineering Research and Design* **54** (a), 167–173.

GUALTIERI, P., CASCIOLA, CM, BENZI, R., AMATI, G. & PIVA, R. 2002 Scaling laws and intermittency in homogeneous shear flow. *Physics of Fluids* **14**, 583.

HUA, J. & LOU, J. 2007 Numerical simulation of bubble rising in viscous liquid. *Journal of Computational Physics* **222** (2), 769–795.

LIU, C., SHEN, J., FENG, J.J. & YUE, P. 2005 Variational approach in two-phase flows of complex fluids: transport and induced elastic stress. *Mathematical Models and Methods in Phase Transitions, Nova Publications* .

OGUZ, H.N. & PROSPERETTI, A. 1993 Dynamics of bubble growth and detachment from a needle. *Journal of Fluid Mechanics* **257** (-1), 111–145.

OHTA, M., IMURA, T., YOSHIDA, Y. & SUSSMAN, M. 2005 A computational study of the effect of initial bubble conditions on the motion of a gas bubble rising in viscous liquids. *International journal of multiphase flow* **31** (2), 223–237.

RYSKIN, G. & LEAL, LG 1984 Numerical solution of free-boundary problems in fluid mechanics. part 1. the finite-difference technique. *Journal of Fluid Mechanics* **148** (-1), 1–17.

TOMIYAMA, A., CELATA, GP, HOSOKAWA, S. & YOSHIDA, S. 2002 Terminal velocity of single bubbles in surface tension force dominant regime. *International journal of multiphase flow* **28** (9), 1497–1519.

UNVERDI, S.O. & TRYGGVASON, G. 1992 A front-tracking method for viscous, incompressible, multi-fluid flows. *Journal of Computational Physics* **100** (1), 25–37.

YUE, P., ZHOU, C. & FENG, J.J. 2010 Sharp-interface limit of the cahn–hilliard model for moving contact lines. *Journal of Fluid Mechanics* **645** (-1), 279–294.